ELSEVIER

Chemical Engineering Journal 84 (2001) 413–428

Chemical Engineering Journal

www.elsevier.com/locate/cej

Application of an integral method to modelling of laminar micromixing

A. Rożeń [a], R.A. Bakker [b], J. Bałdyga [a,*]

[a] *Department of Chemical and Process Engineering, Warsaw University of Technology, ul. Waryńskiego 1, 00-645 Warsaw, Poland*
[b] *DSM Research, Geleen, The Netherlands*

Received 25 April 2000; received in revised form 14 September 2000; accepted 20 September 2000

Abstract

Laminar mixing of very viscous liquids and its effect on the course of parallel chemical reactions have been studied theoretically and experimentally. An existing model of laminar micromixing, based on an integral transformation of material balance equations in a local frame of reference attached to the Lagrangian point has been extended to account for the effects of differential diffusion. Smooth presumed algebraic functions were used to approximate concentration profiles of species in the local frame of reference and to derive ordinary differential equations for the concentration moments of the reactants. In experiments a solution of sodium hydroxide was mixed with a premixture of hydrochloric acid and ethyl chloroacetate in a co-rotating twin-screw extruder in a laminar flow regime. The viscosity of both solutions was increased by adding polyethylenepolypropylene glycol. In the experiments the effects of the screw speed, the extruder throughput, the volume ratio of the mixed reactant solutions and the degree of fill of the extruder on the selectivity of the parallel reactions: acid–base neutralisation and ester hydrolysis, were determined. The model was used to interpret the experimental results.

Keywords: Co-rotating twin-screw extruder; Parallel reactions; Reactive extrusion; Viscous liquids

1. Introduction

Designing devices for mixing of very viscous liquids still constitutes a difficult engineering problem. Extremely high viscosities, high energy input or possibility of thermal degradation of a processed material do not allow mixing of highly viscous liquids to be carried out in the turbulent flow. Therefore, in many industrial applications mixing, especially on the molecular level, occurs at considerably lower rates than in the turbulent case. Slow mixing on the molecular level (micromixing) may affect the course of chemical reactions. It is well known that fast or very fast complex chemical reactions with non-linear kinetics proceeding in an unpremixed feed system can be strongly affected by micromixing [1–4]. However it is not an easy task to predict an outcome of mixing with fast or very fast chemical reactions.

The subject literature indicates that micromixing in the laminar flow proceeds by the deformation of fluid elements and the molecular diffusion of mixture components [5–10]. Viscous deformation generates a new intermaterial surface area, decreases segregation scales in a system and tends to maintain high local gradients of the component concentration. Molecular diffusion, accelerated by deformation, decreases local variations of the component concentration and homogenises the mixture at the molecular level. The rate of the deformation of fluid elements depends on an input of mechanical energy and on an orientation of the intermaterial surface with respect to the principal directions of stretching [8,9]. Differences in such physical properties of the mixed fluids as viscosity and density also affect the rate of deformation [11,12] but micromixing models available in the literature do not account for these effects.

A micromixing model proposed by Ranz [8] and later developed by Ottino et al. [9] assumes that the contacted fluids form stratified structures that are deformed under action of the external flow. To describe the processes of molecular diffusion and chemical reactions, occurring in the lamellar structures, the authors formulate material balance equations in the local frame of reference attached to each structure. The solution of the resulting system of partial differential equations (PDEs) gives the concentration profile and the conversion of each reactant in the lamellar structure. This model neglects mass exchange between the lamellar structure and its surrounding. The initial distribution of the reactants in the lamellar structure is related to the global system composition rather than to local mixing conditions. The solution of the model PDEs requires application of complicated numerical algorithms and a considerable computation power.

* Corresponding author. Tel.: +48-22-6606376; fax: +48-22-8256037.
E-mail address: baldyga@ichip.pw.edu.pl (J. Bałdyga).

1385-8947/01/$ – see front matter
PII: S1385-8947(00)00273-4

Nomenclature

a, b	correlation (46) coefficients
c_i	concentration of reactant i (mol m^{-3})
C_L	centreline distance between screws (m)
d	diameter of injection port (m)
dF	differential contact surface area (m^2)
D	screw diameter (m)
$\overline{\overline{D}}$	rate of deformation tensor (s^{-1})
D_B	screw root diameter (m)
D_i	molecular diffusivity of reactant i (m^2 s^{-1})
f	degree of fill of extruder channel
F_D, F_P	shape factors characterising channel geometry
Fr	Froude number
g	earth acceleration (9.81 m s^{-2})
h	channel depth (m)
k_i	second order reaction rate constants (m^3 mol^{-1} s^{-1})
m	number of screw channels
M_i	zero order concentration moment (mol)
$M_{i,kl}$	second order concentration moment (mol m^2)
$\hat{n}$	direction unit vector
N	screw speed (s^{-1})
p	pressure (Pa)
Δp	die pressure
R_i	reaction rate (mol s^{-1} m^{-3})
Re	Reynolds number
s	striation thickness (m)
t	time (s)
t_D, t_F, t_R	characteristic diffusion, deformation and reaction times (s)
T	screw pitch (m)
$\vec{u}$	velocity in Lagrangian frame (m s^{-1})
u_i	velocity component in Lagrangian frame (m s^{-1})
$\vec{v}$	velocity (m s^{-1})
v_0	local liquid velocity near injection port (m s^{-1})
$\dot{V}$	total extruder throughput (m^3)
$\dot{V}_D$	drag (maximum) flow rate (m^3)
$\dot{V}_i$	volumetric feeding rate (m^3 s^{-1})
$\dot{V}_P$	pressure flow rate (m^3)
w	channel width (m)
X	selectivity
$\vec{X}$	position of material point (m)
z	coordinate in channel direction (m)

Greek letters

α, α_i	rate of deformation (s^{-1})
$\langle\alpha\rangle$	time averaged rate of deformation (s^{-1})
β_B, β_C	initial concentration ratios
γ_B, γ_C	ratios of diffusion coefficients
δ_F	flight clearance (m)
δ_i	half width of gradient profile (m)
δ_{kl}	Kronecker delta
Δ_i	displacement of gradient profile (m)
θ_1, θ_2	characteristic time ratios
κ_i	shape coefficient of gradient profile
$\lambda_{i,k}$	penetration distance (m)
μ	dynamic viscosity (Pa s)
ξ, ξ_i	coordinate in Lagrangian frame (m)
$\vec{\xi}$	position vector in Lagrangian frame (m)
ρ	density (kg m^{-3})
σ_X	average relative difference between the model and the direct numerical solution
φ	screw helix angle (rad)
χ_i	constant dependent on κ_i
ψ	gradient profile function
$\vec{\omega}$	angular velocity of Lagrangian frame (s^{-1})

Subscript

0	initial value

A micromixing model of Bałdyga et al. [10] overcomes these limitations. In this model attention is focused on a spot of one reactant surrounded by other reactants. Material balance equations are formulated in the local frame of reference attached to the centre of mass of the spot (the Lagrangian point) and then converted by means of an integral transformation to a system of ordinary differential equations (ODEs). The solution of these equations gives the rate of growth of the spot volume due to micromixing and the average concentration of the reactants within the spot. Both the mass transfer between the reactive spot and its environment and the effect of local mixing conditions on the characteristic initial scale of the spot are accounted for. This simple model works well when the molecular diffusivities of the reactants do not differ considerably and a small volume of a highly concentrated solution of one reactant is mixed with a large volume of a dilute solution of other reactants. The diffusion coefficients of reactants in the multi-component mixture are in general not equal, often very different, and therefore the concentration fields of these species can evolve differently. For example two species A and B, initially mixed on the molecular scale in a homogeneous mixture that is introduced into a flow, can evolve into different concentration fields $c_A(\vec{x}, t)$ and $c_B(\vec{x}, t)$ due to differences in their diffusion coefficients. Such phenomenon is called "differential diffusion" and can be of special importance in reactive laminar flows, although it has been observed in turbulent flows as well [13]. Therefore, there is a need to extend the application range of the model of Bałdyga et al. [10] by accounting for this effect without, however, significantly complicating the model structure. Such a model may be combined with tools of computational fluid dynamics (CFD) to allow for modelling of micromixing with chemical reaction in very complex flows occurring in industrial mixers and reactors.

An extension of the model [10] is achieved in this paper by the use of an explicit approximation of the local concentration profile of each reactant in the reaction zone and employing an integral method based on ODE for the concentration moments. A similar approach was earlier applied by Tryggvason and Dahm [14] to model combustion processes in isolated strained diffusion layers.

For experimental validation of the new model a reactive tracer method proposed by Bałdyga et al. [10] is applied. In this method, two parallel chemical reactions: acid–base neutralisation and alkaline hydrolysis of an aliphatic ester are run in an unpremixed feed system; the viscosity of the mixed reactant solutions being increased with polyethylenepolypropylene glycol [10,15]. The selectivity of the considered parallel reactions is significantly dependent on mixing conditions in laminar flow for various flow configurations [10,15].

The co-rotating twin-screw extruder (CoTSE) is commonly used in the polymer technology for continuous processing of very viscous materials [16,17]. A self-wiping action of the rotating screws prevents formation of stagnation zones and improves distribution of the minor component in the bulk [18]. An intermaterial surface can be periodically reoriented when passing through the intermeshing region, which significantly improves mixing in a predominantly shear flow in the screw channel [19]. The co-rotating twin-screw extruders offer a great flexibility in choosing screw geometry and operating conditions [20]. Several unit operations: melting, addition of side streams of catalysts or monomers, mixing and chemical reaction, removal of volatises, compression and final extrusion can all be run in a relatively small process volume of CoTSE. Many processes of polymer synthesis and modification such as bulk polymerisation, grafting reactions, interchain co-polymerisation, coupling, branching or even degradation reactions are carried out in CoTSE [21] as well. Some chemical reactions conducted in the extruders are multi-component and diffusion limited reactions with significant differences in diffusion coefficients, e.g. polymerisation of urethanes, which can be influenced by micromixing [22].

There are few experimental studies on reactive laminar micromixing in the extruders. Donn [23] and Wu [24] used a system of competitive-consecutive imidisation reactions, originally developed by Frey [25], proceeding in the polymer melt to study laminar micromixing in CoTSE. They determined the effects of the screw geometry, the extruder throughput and the screw speed on the final selectivity of the imidisation reactions. They observed micromixing effects for this reaction system only for very low screw speeds and extruder throughputs. In the study of Graaf [26] a simple acid–base neutralisation reaction was carried out in CoTSE with a transparent barrel. The length of the reaction zone, marked by a colour change of pH-indicator, was affected by the screw speed and ratio of the viscosities of water–glycerine solutions mixed in the extruder. Graaf [26] also conducted a bulk thermal polymerisation of styrene in the presence of a highly reactive chain transfer agent in a counter-rotating twin-screw extruder. In this method, originally proposed by Meyer and Renken [27], the number average molecular weight of co- and homopolymers depends on the rate of mixing of the chain transfer agent with the bulk flow. The effects of the initial feed segregation, the screw speed and the die resistance on the number average molecular weigh of polymers were determined but no quantitative interpretation of the results was proposed [26].

In the present paper the accuracy and the application range of the proposed model is determined by comparing the selectivity of parallel reactions predicted by the model with the selectivity obtained from a direct numerical solution of the material balance PDEs for a simple well-defined flow. In the next step the model is used to interpret results of micromixing experiments performed in CoTSE by means of the test reaction system of two parallel reactions for a wide range of: the screw speeds, the extruder throughputs and the degrees of fill of the extruder. At the end, the effect of these operating conditions on the average rate of the deformation of the fluid elements in the extruder channel is determined.

2. Model formulation

Mixing of very viscous, Newtonian, incompressible and fully miscible fluids is considered. It is assumed that the flow of the contacted fluids is laminar, hydrodynamically stable and isothermal. The process is described in a local frame of reference attached to the Lagrangian point $\vec{X} = \vec{X}(\vec{X}_0, t)$, being the centre of mass of a fluid element. The fluid element is transported, deformed and rotated by the external flow and can exchange mass with the surrounding. Mixing is accompanied by chemical reactions occurring between a reactant initially contained in the fluid element and other reactants initially present in the environment. The diffusion coefficients of the reactants as well as the rate constants of the chemical reactions are assumed to be unaffected by the mixture composition.

The material balance of the *i*th reactant in the local frame of reference, (ξ_1, ξ_2, ξ_3), reads

$$\frac{\partial c_i}{\partial t} + \sum_{m=1}^{3} \frac{\partial}{\partial \xi_m}(c_i u_m) = D_i \sum_{m=1}^{3} \frac{\partial^2 c_i}{\partial \xi_m^2} + R_i. \tag{1}$$

In the vicinity of the origin of the local frame of reference, $\vec{X} = \vec{X}(\vec{X}_0, t)$, the relative fluid velocity can be approximated by a linear function of the spatial coordinates

$$\vec{u}(\vec{\xi}) = \vec{v}(\vec{X} + \vec{\xi}) - \vec{v}(\vec{X}) - \vec{\omega} \times \vec{\xi} \cong \overrightarrow{\xi} \cdot \mathrm{Grad}\, \vec{u}|_{\vec{\xi}=\vec{0}}, \tag{2}$$

where $\vec{\omega}$ represents the rotation of the coordinate frame. Using the continuity equation for the incompressible fluid flow

$$\frac{\partial u_1}{\partial \xi_1} + \frac{\partial u_2}{\partial \xi_2} + \frac{\partial u_3}{\partial \xi_3} = 0 \tag{3}$$

and Eq. (2) one can rewrite the convection terms in Eq. (1)

$$\frac{\partial c_i}{\partial t} + \sum_{m=1}^{3}\sum_{n=1}^{3}\xi_n \frac{\partial u_m}{\partial \xi_n}\frac{\partial c_i}{\partial \xi_m} = D_i \sum_{m=1}^{3}\frac{\partial^2 c_i}{\partial \xi_m^2} + R_i. \tag{4}$$

Instead of solving a set of Eq. (4) to obtain the exact concentration profiles of reactants and on this basis determine the amount and the distribution of the reactants in the local frame of reference we integrate Eq. (4) with the weight functions "1" and "$\xi_k\xi_1$" over the fluid volume.

These integral transformations produce two equations for the ith reactant:

$$\frac{\mathrm{d}M_i}{\mathrm{d}t} = \int_{-\infty}^{+\infty}\!\!\int\!\!\int R_i \,\mathrm{d}\xi_1\,\mathrm{d}\xi_2\,\mathrm{d}\xi_3, \tag{5}$$

$$\frac{\mathrm{d}M_{i,kl}}{\mathrm{d}t} - \sum_{m=1}^{3}\frac{\partial u_k}{\partial \xi_m}M_{i,ml} - \sum_{n=1}^{3}\frac{\partial u_l}{\partial \xi_n}M_{i,kn} = 2D_i M_i \delta_{kl} + \int_{-\infty}^{+\infty}\!\!\int\!\!\int R_i \xi_k \xi_l \,\mathrm{d}\xi_1\,\mathrm{d}\xi_2\,\mathrm{d}\xi_3. \tag{6}$$

Eqs. (5) and (6) contain two types of transformed, integral variables:

- the zero order moment

$$M_i = \int_{-\infty}^{+\infty}\!\!\int\!\!\int (c_i - c_{i\infty})\,\mathrm{d}\xi_1\,\mathrm{d}\xi_2\,\mathrm{d}\xi_3, \tag{7}$$

- the second order moment

$$M_{i,kl} = \int_{-\infty}^{+\infty}\!\!\int\!\!\int (c_i - c_{i\infty})\xi_k\xi_l \,\mathrm{d}\xi_1\,\mathrm{d}\xi_2\,\mathrm{d}\xi_3. \tag{8}$$

Here $c_{i\infty}$ is the far field concentration of the ith reactant. The rate of change of the zero order moment is equivalent to the rate of consumption or production of the ith reactant. The second order moments characterise the spatial distribution of the ith reactant in the Lagrangian frame of reference. For example, the square root of the ratio $M_{i,kk}/M_i$ can be used as an estimate of the penetration distance of the ith reactant along ξ_k axis, $\lambda_{i,k}$ [10].

The theoretical mechanics states that for any rigid body one can always find three mutually perpendicular main axes of inertia [28]. When the axes of the reference frame, fixed to the centre of mass of the rigid body, are directed along the main axes of inertia all deviatory moments of the body vanish in this frame. The definition of the second order concentration moments, Eq. (8), is formally identical to the definitions of the inertial and deviatory moments of the rigid body. Therefore, in our analysis at any instant of time the coordinate axes (ξ_1, ξ_2, ξ_3) coincide with the main axes of "inertia" of the reactant spot and thus all off-diagonal moments vanish ($M_{i,kl} = 0$ if $k \neq l$). Eq. (6) takes a simpler form that for $k = l$ reads:

$$\frac{\mathrm{d}M_{i,kk}}{\mathrm{d}t} = 2\left(\frac{\partial u_k}{\partial \xi_k}M_{i,kk} + D_i M_i\right) + \int_{-\infty}^{+\infty}\!\!\int\!\!\int R_i \xi_k^2 \,\mathrm{d}\xi_1\,\mathrm{d}\xi_2\,\mathrm{d}\xi_3. \tag{9}$$

The form of Eq. (9) indicates that in the frame of reference translating and rotating with the fluid element the processes of molecular diffusion and chemical reaction can be described, as they would occur in a simple stagnation flow with the deformation rates, α_k, that can vary in time and space, and

$$u_k \cong \left.\frac{\partial u_k}{\partial \xi_k}\right|_{\vec{\xi}=0} \xi_k = \alpha_k \xi_k, \quad k = 1, 2, 3. \tag{10}$$

This interpretation agrees with earlier suggestions of Ranz [8] and Ottino et al. [9].

The deformed fluid element must shrink at least in one direction and extend in the remaining one(s) due to the continuity condition, $\alpha_1 + \alpha_2 + \alpha_3 = 0$, e.g. for $\alpha_1 < 0$ and $\alpha_2, \alpha_3 > 0$ the fluid element takes a shape of a thinning slab. When molecular diffusion proceeds at speeds lower than or comparable to the rate of viscous deformation (only then mechanical mixing is of importance), then the concentration gradients become the highest in the direction of the fastest shrinking, while the fastest growth of the intermaterial surface is observed in the perpendicular direction. Consequently, molecular diffusion becomes significantly accelerated in the direction of the fastest shrinking and slowed down in other directions. Hence, a three-dimensional local concentration field degenerates with time to a one-dimensional one, as illustrated by Bałdyga et al. [10]. Therefore, it can be assumed that a drop of the reactant solution eventually forms an elongated striation and that molecular diffusion proceeds in the direction perpendicular to the symmetry plane of this striation. We attach the origin of a local coordinate system, (ξ_1, ξ_2, ξ_3), to the symmetry plane of the striation and direct it so that ξ_1 axis becomes perpendicular to the symmetry plane, which assures that all off-diagonal concentration moments vanish. When the velocity field in a mixer is known, then the rate of mechanical thinning of the striation along its trajectory, $\vec{X} = \vec{X}(\vec{X}_0, t)$, can be found from [9]

$$\alpha(\vec{X}, t) = -\frac{\partial u_1}{\partial \xi_1} = -\frac{1}{s}\frac{\mathrm{d}s}{\mathrm{d}t} = -\overline{\overline{D}} : \hat{n}\hat{n}, \tag{11}$$

where s is the striation thickness (should not be confused with the ith reactant penetration distance $\lambda_{i,1}$), $\hat{n}$ is the unit vector perpendicular to the symmetry plane of the striation and $\overline{\overline{D}}$ denotes the rate of deformation tensor.

The model equations (5) and (9) contain also integrals dependent on the reaction rate distributions, R_i, that depend on the local concentrations profiles. Tryggvasson and Dahm [14] showed in their study on diffusion controlled combustion that such "reaction integrals" can be well estimated with some simple algebraic approximations of the concentration profiles in the reaction zone. However, the form of

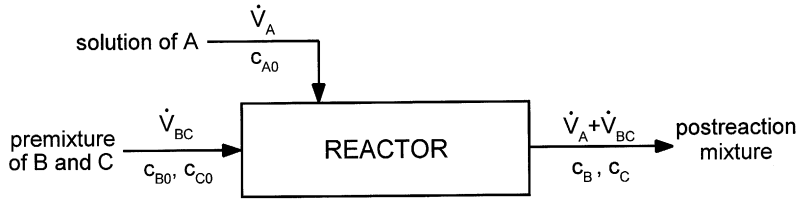

Fig. 1. Schematic representation of an on-line reactor.

these approximations must account for the particular process conditions, e.g. the way of contacting substrates and the reaction kinetics.

In the present work the effect of micromixing on the course of two competitive-parallel chemical reactions of the second order kinetics:

$$A + B \xrightarrow{k_1} P, \tag{12}$$

$$A + C \xrightarrow{k_2} Q, \tag{13}$$

is investigated. The first reaction is very fast and fully controlled by mixing, while the rate at which the second reaction would proceed in the kinetic regime is comparable to rate of laminar micromixing ($k_2 \ll k_1$). A side stream of an A-rich solution is fed into a main stream of a fresh premixture of reagents B and C (with possibly differing diffusion coefficients) in an on-line reactor (Fig. 1). The chemically equivalent amounts of the reactants are applied for simplicity

$$\dot{V}_A c_{A0} = \dot{V}_{BC} c_{B0} = \dot{V}_{BC} c_{C0}. \tag{14}$$

The final selectivity of the parallel reactions (12) and (13) defined as

$$X = \frac{\dot{V}_{BC} c_{C0} - (\dot{V}_A + \dot{V}_{BC}) c_C}{\dot{V}_A c_{A0}}, \tag{15}$$

is directly related to the course of mixing [29]. In the case of infinitely fast mixing in the reactor the selectivity equals zero. When both reactions are fully controlled by mixing, the selectivity reaches the maximum level, which depends on the relation between diffusion coefficients of the reactants, e.g. for $D_A = D_B = D_C$ the maximum selectivity equals 0.5.

To approximate distributions of reactant concentrations in the local frame of reference attached to the elongated striation of the A-rich solution we use expressions similar to those proposed by Tryggvasson and Dahm [14]:

$$c_i = \begin{cases} c_{im} & \text{if } |\xi| \le \Delta_i - \delta_i, \\ (c_{im} - c_{i\infty})[0.5 & \\ -\psi(\xi, \Delta_i, \delta_i, \kappa_i)] + c_{i\infty} & \text{if } \Delta_i - \delta_i \le |\xi| \le \Delta_i + \delta_i, \\ c_{i\infty} & \text{if } |\xi| \le \Delta_i + \delta_i, \end{cases} \tag{16}$$

$$\psi(\xi, \Delta_i, \delta_i, \kappa_i) = \frac{\sqrt{\kappa_i + 1}}{4} \frac{(2\kappa_i - 1)(\xi - \Delta_i)^3 + 3\delta_i^2(\xi - \Delta_i)}{[\kappa_i(\xi - \Delta_i)^2 + \delta_i^2]^{3/2}} \quad \text{for } i = A, B, C. \tag{17}$$

To simplify notation symbol ξ_1 is replaced by ξ in Eqs. (16) and (17) and following ones. Parameters Δ_i and δ_i represent the position of the inflexion points and the half width of the profile (Fig. 2). The ith reactant concentration at the symmetry plane of the slab is denoted by c_{im}, while its far field value by $c_{i\infty}$. The shape of the concentration profile depends on the value of the coefficient, κ_i (Fig. 3).

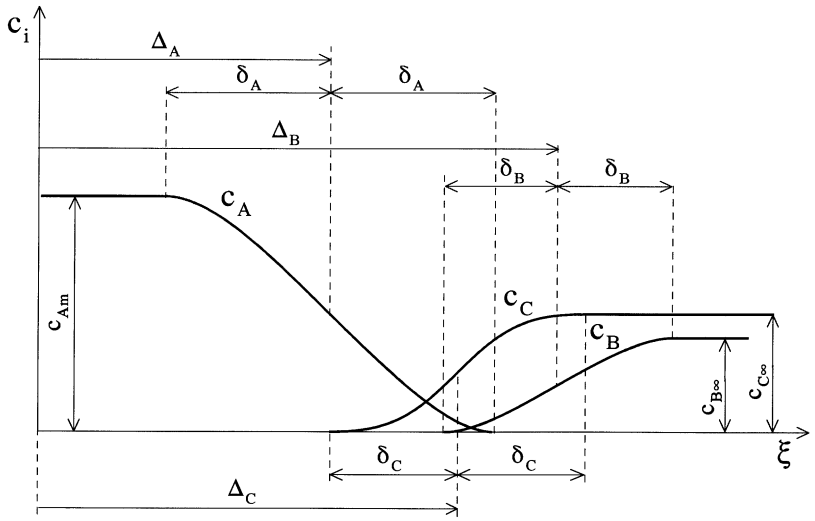

Fig. 2. Approximations of local concentration profiles of reactants.

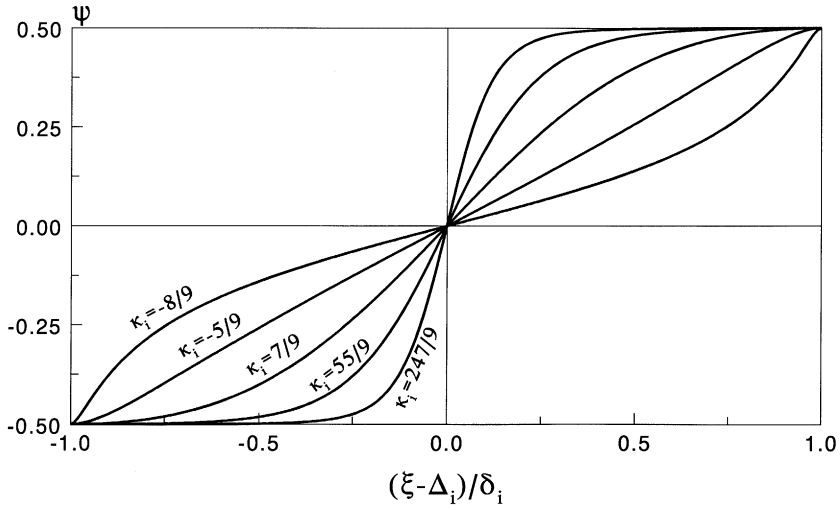

Fig. 3. Gradient profile function.

When Eqs. (16) and (17) are combined with Eqs. (7) and (8) the following expressions arise:

$$M_i = 2(c_{im} - c_{i\infty})\Delta_i \, \mathrm{d}F, \tag{18}$$

$$M_{i,11} = 2(c_{im} - c_{i\infty})\Delta_i \left(\frac{\Delta_i^2}{3} + \chi_i \delta_i^2 \right) \mathrm{d}F, \tag{19}$$

where

$$\chi_i = \begin{cases} \dfrac{\kappa_i + 3}{2\kappa_i^2} - \dfrac{3\sqrt{\kappa_i + 1}}{2|\kappa_i|^{5/2}} \arcsin\sqrt{|\kappa_i|} & \text{for } -1 < \kappa_i < 0, \\ \frac{1}{5} & \text{for } \kappa_i = 0, \\ \dfrac{\kappa_i + 3}{2\kappa_i^2} - \dfrac{3\sqrt{\kappa_i + 1}}{4\kappa_i^{5/2}} \ln \dfrac{\sqrt{\kappa_i + 1} + \sqrt{\kappa_i}}{\sqrt{\kappa_i + 1} - \sqrt{\kappa_i}} & \text{for } \kappa_i > 0. \end{cases} \tag{20}$$

Evolution of the reactant contact surface area, dF, can be found by combining the continuity condition, $s\,\mathrm{d}F =$ constant, with Eq. (11)

$$\mathrm{d}F = \mathrm{e}^{\langle\alpha\rangle t} \, \mathrm{d}F_0, \qquad \langle\alpha\rangle = \frac{1}{t}\int_0^t \alpha(\vec{X}, t') \, \mathrm{d}t'. \tag{21}$$

Introduction of Eqs. (18)–(21) into the Eqs. (5) and (9) gives

$$\Delta_i \frac{\mathrm{d}c_{im}}{\mathrm{d}t} + (c_{im} - c_{i\infty}) \left(\frac{\mathrm{d}\Delta_i}{\mathrm{d}t} + \alpha \Delta_i \right) = -\int_0^{+\infty} (k_1 c_\mathrm{A} c_\mathrm{B} + k_2 c_\mathrm{A} c_\mathrm{C}) \, \mathrm{d}\xi, \tag{22}$$

$$\Delta_i \left(\frac{\Delta_i^2}{3} + \chi_i \delta_i^2 \right) \frac{\mathrm{d}c_{im}}{\mathrm{d}t} + (c_{im} - c_{i\infty}) \times \left[(\Delta_i^2 + \chi_i \delta_i^2) \frac{\mathrm{d}\Delta_i}{\mathrm{d}t} + 2\chi_i \Delta_i \delta_i \frac{\mathrm{d}\delta_i}{\mathrm{d}t} + \alpha \Delta_i (\Delta_i^2 + 3\chi_i \delta_i^2) \right] = 2D_i (c_{im} - c_{i\infty}) \Delta_i - \int_0^{+\infty} (k_1 c_\mathrm{A} c_\mathrm{B} + k_2 c_\mathrm{A} c_\mathrm{C}) \xi^2 \, \mathrm{d}\xi. \tag{23}$$

In the initial stage of the process the system of Eqs. (16), (17), (22) and (23) is solved for the half width, δ_i, and the displacement, Δ_i, of the profiles with the initial conditions:

$$\Delta_i = \frac{s_0}{2}, \qquad \delta_i = 0, \quad i = \mathrm{A}, \mathrm{B}, \mathrm{C}. \tag{24}$$

The species concentrations at the origin and in the environment remain constant:

$$c_{\mathrm{A}m} = c_{\mathrm{A}0}, \quad c_{\mathrm{A}\infty} = 0, \quad c_{\mathrm{B}m} = 0, \quad c_{\mathrm{B}\infty} = c_{\mathrm{B}0}, \quad c_{\mathrm{C}m} = 0, \quad c_{\mathrm{C}\infty} = c_{\mathrm{C}0}. \tag{25}$$

As the mixing proceeds, the half width of the profile, δ_i, increases and eventually becomes equal to the displacement, Δ_i. After that moment Δ_i is replaced with δ_i in Eqs. (16), (17), (22) and (23), while the concentration level at the origin, c_{im}, is parameterised. The coefficients, κ_i, when once chosen for the specific case remain unchanged during computation; the problem of selecting a proper value of κ_i is discussed later in this chapter.

Reactions (12) and (13) proceed until there is no more substrate A left in the striation. Therefore, in the present work ODEs (22) and (23) were integrated until $c_{\mathrm{A}m} = 0$. A fourth-order Runge–Kutta algorithm with an automatic step size correction was used to integrate ODEs (22) and (23). To assure that the first reaction, Eq. (12), was fully controlled by micromixing the value of the reaction rate constant, k_1, was gradually increased until its value had no effect on the computed selectivity.

The accuracy of the present model formulation has been tested by comparing its predictions with results of a direct numerical solution of a system of three material balance equations

$$\frac{\partial c_i}{\partial t} - \alpha\xi \frac{\partial c_i}{\partial \xi} = D_i \frac{\partial^2 c_i}{\partial \xi^2} + R_i,$$

$$R_i = \begin{cases} -k_1 c_A c_B - k_2 c_A c_C & \text{if } i = A, \\ -k_1 c_A c_B & \text{if } i = B, \\ -k_2 c_A c_C & \text{if } i = C, \end{cases} \quad (26)$$

with initial and boundary conditions:

$$c_A(\xi, 0) = \begin{cases} c_{A0} & \text{if } |\xi| < \frac{1}{2}s_0 \\ 0 & \text{if } |\xi| \geq \frac{1}{2}s_0 \end{cases}, \quad c_A(\xi \to \pm\infty, t) = 0, \quad (27)$$

$$c_i(\xi, 0) = \begin{cases} 0 & \text{if } |\xi| < \frac{1}{2}s_0 \\ c_{i0} & \text{if } |\xi| \geq \frac{1}{2}s_0 \end{cases},$$
$$c_i(\xi \to \pm\infty, t) = c_{i0}, \qquad i = B, C. \quad (28)$$

A numerical algorithms group (NAG) Fortran library routine, employing a method of lines and an implicit time integration formula, was applied to solve PDEs (26). The reaction rate constant, k_1, and the distance between space boundaries (range of ξ) were increased to such levels that their effect on the computational results became negligible. The computations were performed on a Cray J932 supercomputer.

To present the computation results in a convenient way the following dimensionless parameters were introduced:

- initial concentration ratio

$$\beta_i = \frac{c_{i0}}{c_{A0}}, \quad (29)$$

- diffusion coefficient ratio

$$\gamma_i = \frac{D_i}{D_A}, \quad (30)$$

- first characteristic time ratio

$$\theta_1 = \frac{t_F}{t_R}, \quad (31)$$

- second characteristic time ratio

$$\theta_2 = \frac{t_D}{t_F}. \quad (32)$$

The characteristic time scales used in definition (31) and (32) represent:

- characteristic diffusion time

$$t_D = \frac{M_{A,11}(0)}{M_A(0) D_A} = \frac{s_0^2}{12 D_A}, \quad (33)$$

- characteristic deformation time

$$t_F = \frac{1}{\langle\alpha\rangle}, \quad (34)$$

- characteristic reaction time

$$t_R = \frac{1}{k_2 c_{A0}}. \quad (35)$$

The results of the direct numerical solution, presented in Fig. 4, indicate that the rate of mechanical mixing has strong effect on the course of the parallel reactions (12) and (13). The slower mechanical mixing (higher θ_1) is comparing to the reaction rate, the better chance for the second (slower)

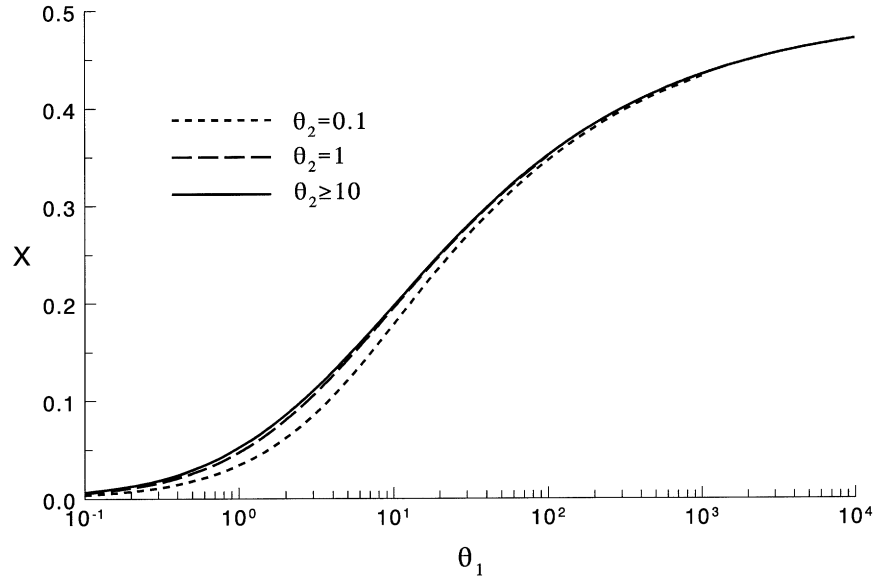

Fig. 4. Final selectivity of parallel reactions; $\beta_B = \beta_C = \frac{1}{24}$, $\gamma_B = \gamma_C = 1$.

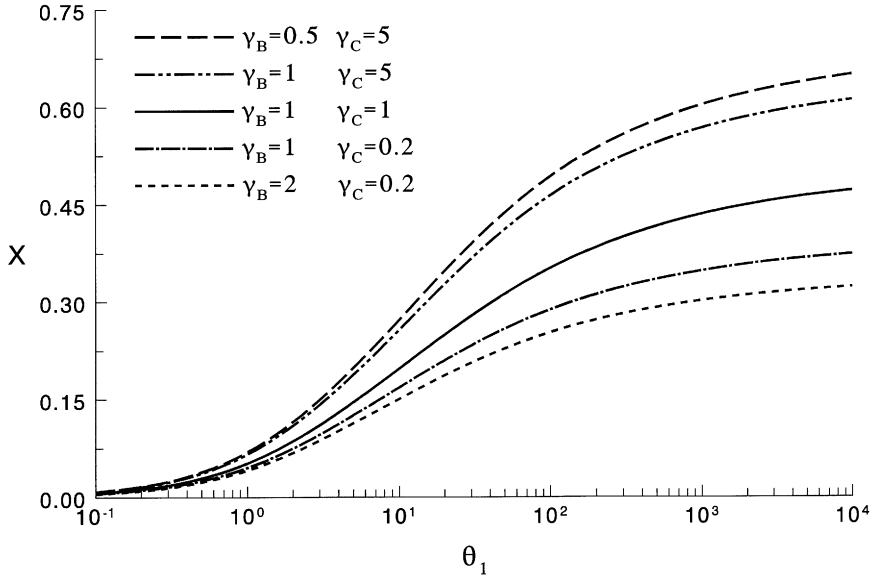

Fig. 5. Final selectivity of parallel reactions; $\beta_B = \beta_C = \frac{1}{24}$, $\theta_2 \geq 10$.

reaction to proceed. Increasing the second time ratio, θ_2, at $\theta_1 =$ constant also elevates the final selectivity, X, but this effect becomes negligible for $\theta_2 \geq 10$, when the molecular diffusion of reactants is relatively very slow comparing to the deformation rate. For $\theta_2 < 1$ the initial scale of segregation significantly affects the final selectivity, X, but this case reflects no mechanical mixing; moreover in this case the assumption that the spot of the reactant of an arbitrary shape becomes an elongated striation is no longer correct.

When the coefficient of the molecular diffusion of reactant C is significantly decreased (increased) the transport of C towards the A-rich zone is slowed down (accelerated) and consequently the conversion of C in the whole process decreases (increases). This explains the results of the direct numerical solution, as shown in Fig. 5.

Fig. 6 refers to the case when the initial concentration of reactant A is only two times higher than the concentration of the reactants initially present in the environment; $\beta_B = \beta_C = \frac{1}{2}$. This allows for an even better penetration of reagent C into the A-rich zone if $\gamma_B = \frac{1}{5}\gamma_C = 1$, than in the case when $\beta_B = \beta_C = \frac{1}{24}$ and $\gamma_B = \frac{1}{5}\gamma_C = 1$. As the result, the final selectivity, X, is higher for $\beta_B = \beta_C = \frac{1}{2}$ than for $\beta_B = \beta_C = \frac{1}{24}$. When γ_C is decreased, A is rather consumed in

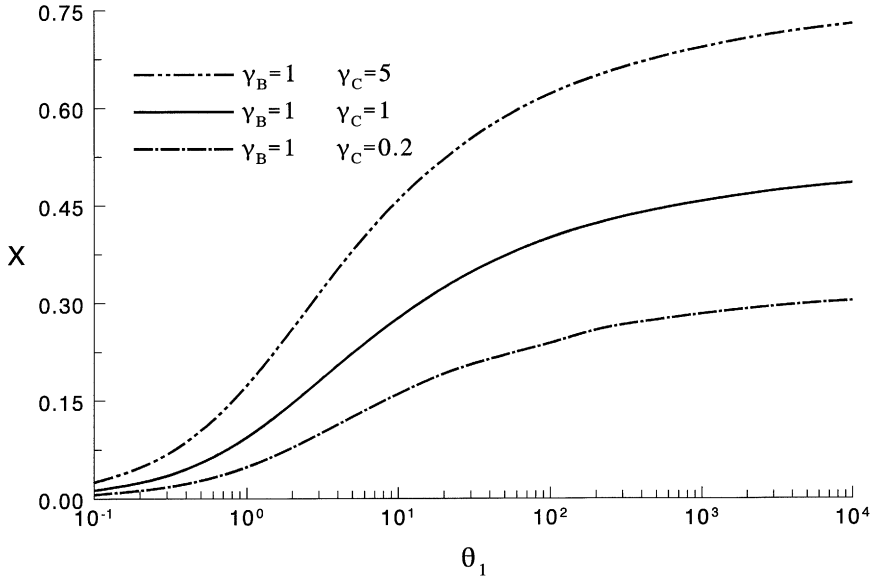

Fig. 6. Final selectivity of parallel reactions; $\beta_B = \beta_C = \frac{1}{2}$, $\theta_2 \geq 10$.

Table 1
Coefficients κ_A and κ_B giving the minimum of σ_X for $\gamma_B = 1$, $\theta_2 = 10$ and $\kappa_C = \frac{7}{9}$

	γ_C					
	0.2	1	2	3	4	5
$\beta_B = \beta_C = \frac{1}{24}$						
$\kappa_A = \kappa_B$	−0.70	−0.37	–	0.93	–	3.0
σ_X	0.015	0.005	–	0.002	–	0.006
$\beta_B = \beta_C = \frac{1}{8}$						
$\kappa_A = \kappa_B$	−0.74	−0.46	−0.02	0.49	0.98	1.44
σ_X	0.009	0.011	0.009	0.008	0.007	0.008
$\beta_B = \beta_C = \frac{1}{4}$						
$\kappa_A = \kappa_B$	−0.78	−0.50	−0.13	0.20	0.47	0.61
σ_X	0.004	0.018	0.016	0.013	0.010	0.010
$\beta_B = \beta_C = \frac{1}{2}$						
$\kappa_A = \kappa_B$	−0.81	−0.50	−0.21	−0.10	0.06	0.05
σ_X	0.023	0.033	0.024	0.015	0.014	0.011

reaction with B before C can penetrate the A-rich zone and the final selectivity may decrease.

The model coefficients, κ_i, were determined by comparing the selectivities obtained from the solution of PDEs (26) and the solution of ODEs (22) and (23). For given values of the concentration ratio, β_i, the diffusivity ratio, γ_i, and the second characteristic time ratio, $\theta_2 = 10$, the selectivities were computed for five values of the first characteristic time ratio, $\theta_{1,i}$ (=0.1, 1, 10, 10^2, 10^3, 10^4). Then an average relative difference between the solution of ODEs (23) — X_{model} and the solution of PDEs (26) — X was calculated from equation

$$\sigma_X = \left\{ \frac{1}{n} \sum_{i=1}^{n} \left[1 - \frac{X_{model}(\theta_{1,i})}{X(\theta_{1,i})} \right]^2 \right\}^{1/2} . \quad (36)$$

Table 1 reports the values of the model coefficients, κ_A and κ_B, that give the minimum value of σ_X, in the case when $\beta_B = \beta_C$, $\gamma_B = 1$ and $\kappa_C = \frac{7}{9}$.

Low values of σ_X reported in Table 1 show that a proper selection of the coefficients, κ_i, gives a very good fit of the model results, X_{model}, to the results of the direct solution of PDEs (26), X, for the characteristic time ratio θ_1 ranging from 0.1 to 10^4.

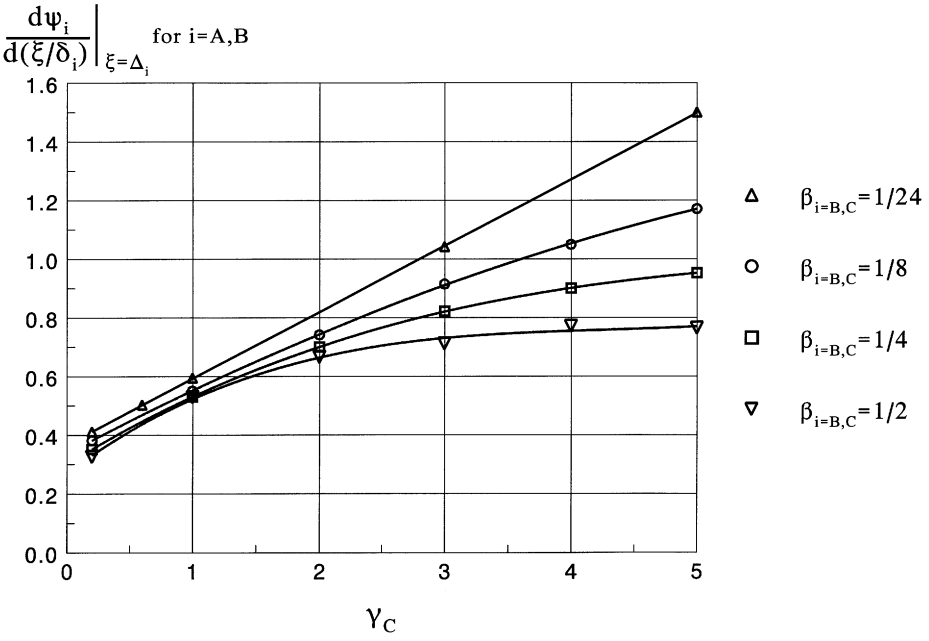

Fig. 7. Slope of a concentration profile at the inflection point giving the best accuracy of the model; $\gamma_B = 1$, $\theta_2 \geq 10$.

When there is a need to perform computations for intermediate conditions one can interpolate the values of κ_A and κ_B from Fig. 7. In this figure the value of the first derivative of the normalised concentration profile of reactants A and B at the inflection point

$$\left.\frac{d\psi}{d(\xi/\delta_i)}\right|_{\xi=\Delta_i} = \frac{3}{4}\sqrt{\kappa_i + 1} \tag{37}$$

was plotted vs. the diffusivity ratio, γ_C, using data reported in Table 1. The interpolation is very simple for the lowest concentration ratios, β_B and β_C, when the slope at the inflection point becomes a linear function of γ_C.

When the molecular diffusivities of all the reactants differ from each other then the coefficients κ_A and κ_B should be adjusted separately by fitting the model results to the direct numerical solution of material balance equation (26). In such a case their values reported in Table 1 can be used as the first approximation. However, for $0.5 \leq \gamma_B \leq 2$ and $0.2 \leq \gamma_C \leq 5$ one can safely apply the values of κ_A and κ_B found for $\gamma_B = 1$. For example, when $\beta_B = \beta_C = \frac{1}{24}$, $\gamma_B = 2$, $\gamma_C = 0.2$, $\theta_2 = 10$ and $\kappa_C = \frac{7}{9}$ the minimum of σ_X equal 0.011 is obtained for $\kappa_A = -0.70$ and $\kappa_B = -0.84$. In the same conditions but for $\kappa_A = \kappa_B = -0.70$ σ_X equals 0.021, which is still a small value. For the same reason the coefficients κ_A and κ_B reported in Table 1 can be used for $\theta_2 < 10$.

The earlier model [10], would give $\sigma_X \cong 0.3$ for $\beta_B = \beta_C = \frac{1}{24}$, $\gamma_B = 1$, $\gamma_C = 0.2$ and $\sigma_X \cong 0.2$ for $\beta_B = \beta_C = \frac{1}{24}$, $\gamma_B = 1$, $\gamma_C = 5$. Only in the case of equal molecular diffusivities of the reactants and for high concentrations of reactant A ($\beta_B \ll 1$, $\beta_C \ll 1$) that model works well.

Similarly to its earlier version, the new model requires far less computation power than it is necessary to obtain the direct numerical solution of partial differential material balance equations. This allows an easy incorporation of the model into a larger computation project involving, e.g., CFD simulation of the complex flow field, determination of the history of deformation for a large population of fluid elements and computation of the conversion or selectivity of chemical reactions occurring between the mixed reactants.

3. Experimental method

A system of two parallel chemical reactions of the second order kinetics:

$$NaOH + HCl \xrightarrow{k_1} NaCl + H_2O \tag{38}$$

$$NaOH + CH_2ClCOOC_2H_5 \xrightarrow{k_2} CH_2ClCOONa + C_2H_5OH \tag{39}$$

and a neutral viscosity increasing agent added to aqueous solutions of the reactants — polyethylenepolypropylene glycol (Breox 75W 18000) — were used to study experimentally laminar micromixing in a co-rotating twin-screw extruder. Neutralisation of hydrochloric acid (reactant B) with sodium hydroxide (reactant A) is instantaneous ($k_1 = 10^{11}\,dm^3\,mol^{-1}\,s^{-1}$) and completely controlled by mixing. The reaction rate constant of alkaline hydrolysis of ethyl chloroacetate (reactant C), k_2, equals $33.2\,dm^3\,mol^{-1}\,s^{-1}$ at 25°C in aqueous solutions of the viscosity increasing agent [15]. When the average NaOH concentration in the reacting mixture is close to $10\,mol\,m^{-3}$ the rate of ester hydrolysis is of the same order of magnitude as the typical rate of laminar micromixing [10]. It has been proven experimentally that when a solution of base is mixed in the laminar flow with a premixture of acid and ester, the selectivity of the test reactions, Eqs. (38) and (39), significantly depends on mixing conditions in: a batch, semi-batch and on-line mixers [10,15].

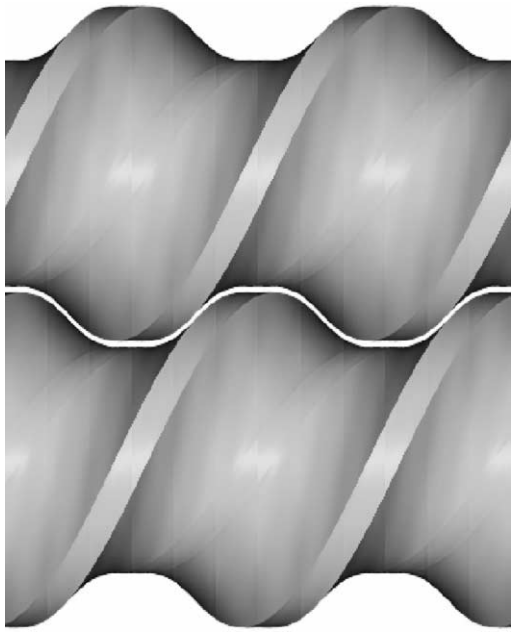

Fig. 8. Intermeshing screw elements of CoTSE.

The extruder used in the experiments had two co-rotating and intermeshing screws mounted in a transparent plexiglas barrel. Each screw comprised 23 double-flighted transport elements presented in Fig. 8. The geometrical parameters were as follows: the screw diameter, $D = 0.0246\,m$, the screw root diameter, $D_B = 0.0166\,m$, the flight clearance, $\delta_F = 0.002\,m$, the screw pitch, $T = 0.037\,m$ and the centreline distance between the screws, $C_L = 0.021\,m$.

Two reactant solutions were continuously fed into the extruder (Fig. 9). The diluted solution of HCl and $CH_2ClCOOC_2H_5$ was fed under atmospheric pressure to the main feed throat and then conveyed by the rotating screws. The concentrated NaOH solution was pumped directly into the intermeshing region of the screws via a small port of 1 mm diameter localised downstream. A syringe pump was used to secure the constant flow rate of the side stream. Equivalent numbers of moles of reactants were always

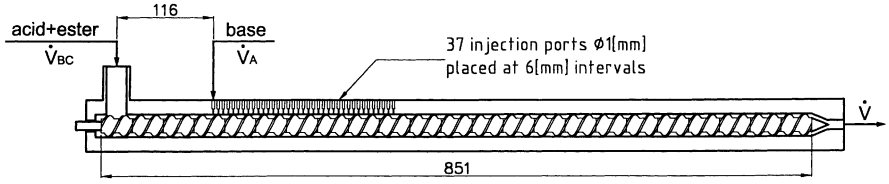

Fig. 9. Diagram of a co-rotating twin-screw extruder.

mixed (Eq. (14)). The viscosity of the reactant solutions was increased up to 0.18 or 0.27 Pa s to obtain a laminar flow regime in the extruder. The temperature of both feeding streams was kept at 25°C. The out-flowing liquid mixture, collected during a specified time period, was weighted to determine the actual extruder throughput. A valve mounted at the extruder discharge was used to adjust the throughput. After the steady state of the process was reached several samples of the out-flowing mixture were taken and analysed by means of high pressure liquid chromatography (HPLC).

4. Results and discussion

The co-rotating twin-screw extruders usually operate in the starved feeding regime, when some part of the extruder channel is only partially filled with the processed material. There is no pressure built-up in the partially filled section, which allows an easy addition of side streams of a monomer or a catalyst and easy removal of volatises via openings in the barrel. Mixing of the side streams with the matrix liquid is mainly conducted in a following completely filled section. However, some part of the mixing process can actually take place in the feeding section and may affect the course of chemical reactions occurring between the reactants. Therefore, in the present work micromixing is investigated both in the completely and partially filled extruder channel.

When the extruder channel is completely filled, then according to a simplified flow theory commonly used in the extruder technology [30] the extruder throughput, $\dot{V}$, is the superposition of the drag flow, $\dot{V}_D$, and the pressure flow, $\dot{V}_P$:

$$\dot{V} = \dot{V}_D - \dot{V}_P = \frac{1}{2} m F_D h w U - m F_P \frac{h^3 w}{12} \frac{1}{\mu} \frac{\partial p}{\partial z}. \tag{40}$$

The drag flow, $\dot{V}_D$, is proportional to the relative barrel velocity:

$$U = \pi D N \cos\varphi, \qquad \varphi = \operatorname{arctg}\left[\frac{T}{\pi D}\right]. \tag{41}$$

The pressure flow, $\dot{V}_P$, is proportional to the pressure gradient along the screw channel, $\partial p/\partial z$, and it is inversely proportional to the material viscosity, μ. The maximum extruder throughput is achieved when $\partial p/\partial z = 0$ and is equal to the drag flow, $\dot{V}_D$. Measurements conducted for CoTSE used in the micromixing experiments showed that the extruder throughput, $\dot{V}$, depends on the die pressure, Δp, the screw speed, N, and the liquid viscosity, μ, according to the following experimental correlation

$$\dot{V} = \dot{V}_D - \dot{V}_P = 0.139 N D^3 - 2.27 \times 10^{-6} D^3 \frac{\Delta p}{\mu}. \tag{42}$$

Results of numerical simulations of the incompressible, Newtonian and creeping flow in CoTSE, performed by Denson and Hwang [31], indicate that the dimensionless velocity profile in the screw channel, $\vec{v}/U$, depends on the ratio of the pressure flow and the drag flow, $\dot{V}_P/\dot{V}_D$. Therefore, the rate of deformation of fluid elements, α, related to the velocity field via Eq. (11), should depend on the screw speed, N and the ratio $\dot{V}_P/\dot{V}_D$ (or $\dot{V}/\dot{V}_D$).

Based on these conclusions several series of experiments with the test reactions, Eqs. (38) and (39), were conducted in the completely filled extruder in such a way that in each series the ratio $\dot{V}/\dot{V}_D$ was kept constant for a wide range of the screw speeds. In these experiments the Reynolds number

$$Re = \frac{U h \rho}{\mu} \tag{43}$$

ranged between 0.4 and 5. In the first three series of experiments the ratio of the feeding flows, $\dot{V}_{BC}/\dot{V}_A$, was equal to 24 while the initial concentrations of the reactants (A = NaOH, B = HCl, C = $CH_2ClCOOC_2H_5$) were as follows $\frac{1}{24} c_{A0} = c_{B0} = c_{C0} = 10\,\mathrm{mol\,m^{-3}}$. In the following three series the value of $\dot{V}_{BC}/\dot{V}_A$ was decreased to 7.33 but the amounts of the mixed reactants were unchanged because $\frac{1}{7.33} c_{A0} = c_{B0} = c_{C0} = 10.9\,\mathrm{mol\,m^{-3}}$.

Experimental results shown in Fig. 10 indicate that there is a strong dependence of the final selectivity of the parallel reactions, X, upon the screw speed, N. In all six series of experiments the selectivity decreases with the increasing screw speed. The selectivity also depends on the ratio of the actual flow rate and the maximum flow rate, $\dot{V}/\dot{V}_D$. A comparison of the selectivities obtained for the similar screw speeds but different ratios $\dot{V}/\dot{V}_D$ shows that the selectivity is higher for lower values of $\dot{V}/\dot{V}_D$, equivalent to higher contribution of the pressure flow, $\dot{V}_P$, into the total flow. Finally it can be observed that the selectivity can be changed without changing both the amounts of the mixed reactants and the flow field. As it is shown in Fig. 10 the experimental points obtained for $\dot{V}_{BC}/\dot{V}_A = 24$ lay higher than those determined for $\dot{V}_{BC}/\dot{V}_A = 7.33$ provided that the values of N and $\dot{V}/\dot{V}_D$ are similar for the compared points.

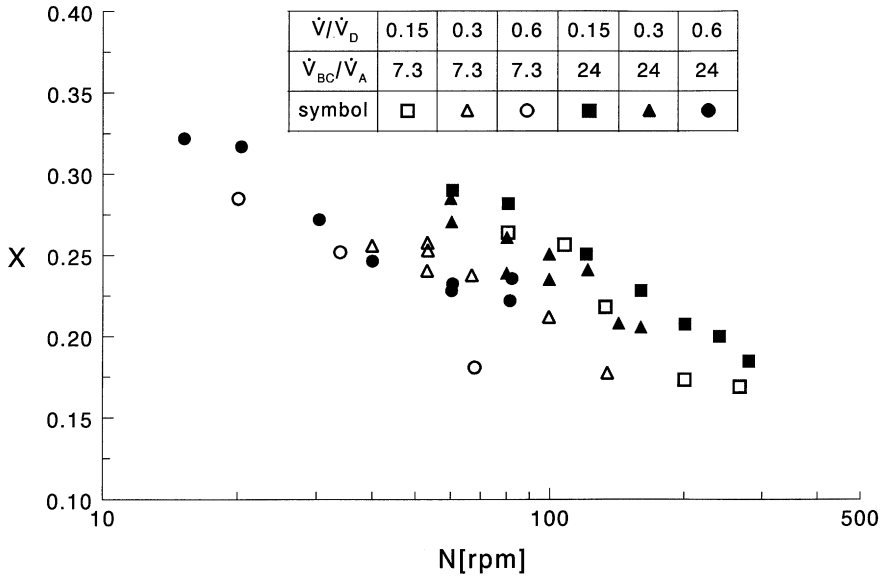

Fig. 10. Final selectivity of parallel reactions determined experimentally for fully filled CoTSE.

The model of laminar micromixing, described in the previous chapter, was applied to interpret quantitatively the experimental results. Similarly as in the earlier work [10], it was assumed in computations that the base solution injected into the main stream is swept by the rotating screws from the injection port and forms a thin elongated ribbon surrounded by the fresh acid and ester solution. The molecular diffusivities of the reactants, were found from correlations reported by Bałdyga et al. [10]: $D_{\mathrm{NaOH}} = 8.6 \times 10^{-10}$ (6.7×10^{-10}) $\mathrm{m^2\,s^{-1}}$, $D_{\mathrm{HCl}}/D_{\mathrm{NaOH}} \cong 1.5$ (1.7) and $D_{\mathrm{ester}}/D_{\mathrm{NaOH}} \cong 0.22$ (0.21); the first value refers to $\mu = 0.18$ Pa s, the second one in parentheses refers to $\mu = 0.27$ Pa s. The initial striation thickness, s_0, was related to the volumetric flow rate of the side stream via the continuity equation

$$\dot{V}_{\mathrm{A}} = \frac{\dot{V}_{\mathrm{D}}}{1 + \dot{V}_{\mathrm{BC}}/\dot{V}_{\mathrm{A}}} \frac{\dot{V}}{\dot{V}_{\mathrm{D}}} = d s_0 v_0, \tag{44}$$

where d (=1 mm) is the diameter of the injection port and v_0 the local liquid velocity near this port. According to Eq. (42) $\dot{V}_{\mathrm{D}} \sim ND^3$ and if $\dot{V}/\dot{V}_{\mathrm{D}} =$ constant the time average of v_0 should be proportional to ND. In these circumstances the initial striation thickness fulfils the relation

$$s_0 \sim \frac{\dot{V}_{\mathrm{A}}}{dDN} \sim \frac{D^2}{d(1 + \dot{V}_{\mathrm{BC}}/\dot{V}_{\mathrm{A}})} \frac{\dot{V}}{\dot{V}_{\mathrm{D}}}. \tag{45}$$

Hence, if additionally $\dot{V}_{\mathrm{BC}}/\dot{V}_{\mathrm{A}} =$ constant then $s_0 =$ constant. This allowed applying a single value of s_0 for all the experimental points obtained for the same values of $\dot{V}/\dot{V}_{\mathrm{D}}$ and $\dot{V}_{\mathrm{BC}}/\dot{V}_{\mathrm{A}}$ (one series of experiments). The values of s_0 used in the model computations ranged from 0.05 to 5 mm. The average rate of deformation of fluid elements in the reaction zone, $\langle\alpha\rangle$, was determined for each experimental point separately by comparing the computed selectivity to the measured one. Fig. 11 presents the values of $\langle\alpha\rangle/N$ determined from the experimental points reported in Fig. 10. Only when the striation thickness was reduced by deformation below the limiting values given in Table 2 molecular diffusion became accelerated and chemical reactions could proceed at noticeable rates.

Table 2
Limiting values of the initial striation thickness, s_0

	$\dot{V}/\dot{V}_{\mathrm{D}}$		
	0.15	0.3	0.6
s_0 (mm)	0.25	0.5	1

Fig. 11 shows that the ratio of the average rate of deformation, $\langle\alpha\rangle$, in the reaction zone and the screw speed, N, depends on the ratio of the actual throughput to the maximum flow, $\dot{V}/\dot{V}_{\mathrm{D}}$ and the screw speed; the higher values of $\dot{V}/\dot{V}_{\mathrm{D}}$ and N, the higher value of $\langle\alpha\rangle/N$. The correlation between these three quantities can be proposed in the following form:

$$\langle\alpha\rangle = aN^b, \tag{46}$$

where the coefficients a and b depend on $\dot{V}/\dot{V}_{\mathrm{D}}$ as shown in Table 3.

Table 3
Coefficients a and b in correlation (46) found by the least square method

	$\dot{V}/\dot{V}_{\mathrm{D}}$		
	0.15	0.3	0.6
a	0.025	0.046	0.178
b	1.91	1.99	2.06

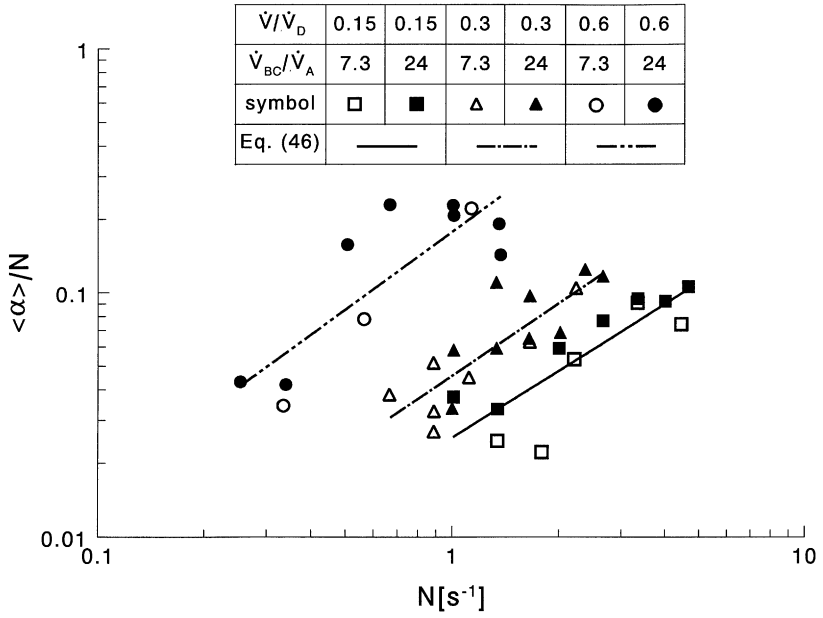

Fig. 11. Average rate of deformation identified for a fully filled section of CoTSE.

When the procedure of fitting of the computed selectivities to the measured ones was repeated for the values of the initial striation thickness smaller that those given in Table 2, it was found that decreasing s_0 decreases the dimensionless rate of deformation, $\langle\alpha\rangle/N$. Therefore the values of $\langle\alpha\rangle/N$ plotted in Fig. 11 are the maximum ones.

When a section of the extruder channel is partially filled, transport of the processed material occurs by the drag flow. However, the actual throughput, $\dot{V}$, is smaller than the maximum drag flow capacity, $\dot{V}_D$ [20]:

$$\dot{V} = f\dot{V}_D, \tag{47}$$

where f is the local degree of fill of the screw channel ($0 < f \leq 1$) defined as the ratio of the liquid volume to the free volume between the screws and the barrel. The flow field in the partially filled channel depends on the system geometry and on the magnitude of viscous, gravity and inertia forces acting on the fluid elements. Therefore, the average rate of deformation of the fluid elements, $\langle\alpha\rangle$, divided by the screw speed, N, should depend on the degree of fill, f, the Reynolds number, Re, and the Froude number, which is defined as

$$Fr = \frac{U^2}{gh}. \tag{48}$$

When the gravity forces dominate over the viscous forces, $Fr \ll Re$, the liquid stays at the channel bottom and it is pushed by the screw flight. When, however, the magnitude of the viscous forces is increased so that $Fr/Re > 0.1$ the liquid is lifted up from the channel bottom and a liquid layer is formed at the screw flights [26,30]. This phenomenon was observed during experiments conducted in the underfed extruder. In these experiments the side stream (NaOH solution) was injected into the long partially filled channel section. The ratio of the flow rates, $\dot{V}_{BC}/\dot{V}_A$, was kept close to 24 while the initial reactant concentrations were set at $\frac{1}{24}c_{A0} = c_{B0} = c_{C0} = 10\,\mathrm{mol\,m^{-3}}$. The selectivity of the test reactions, Eqs. (38) and (39), was determined for a wide range of the degrees of fill ($0.05 < f < 0.5$) and for three screw speeds: $N = 80\,\mathrm{rpm}$ ($Re = 1.5$, $Fr/Re = 0.15$), $N = 120\,\mathrm{rpm}$ ($Re = 2.2$, $Fr/Re = 0.23$) and $N = 180\,\mathrm{rpm}$ ($Re = 3.3$, $Fr/Re = 0.34$).

Experimental results presented in Fig. 12 indicate that the final selectivity, X, increases when the degree of fill, f, is decreased and the screw speed, N, is constant. Poor mixing for small degrees of fill is likely to be caused by reduction of the boundary surface area at which the momentum flux, created by the rotation of screws with respect to each other and to the stationary barrel, is applied to the processed liquid. The smaller amount of the stress is applied at the liquid boundaries, the slower deformation of liquid elements is observed. In the similar manner one can explain why in most cases increasing the screw speed improves mixing and decreases the selectivity when the degree of fill is kept constant (Fig. 12). It should be noted, however, that for $f < 0.08$ the final selectivity determined for $N = 80\,\mathrm{rpm}$ is lower than the selectivity measured for $N = 120\,\mathrm{rpm}$. This may have been caused by the flow disturbances observed at $N = 80\,\mathrm{rpm}$ when some liquid smeared on the top of the barrel was dripping to the channel bottom before it could be wiped by the incoming screw flight. At the higher screw speeds the flow disturbances were observed for $f > 0.2$.

The micromixing model was used to determine the average rate of deformation of fluid elements in the partially filled channel. It was assumed in the computations that the base solution injected into the partially filled zone forms a thin striation over a thick layer of the acid and ester solution

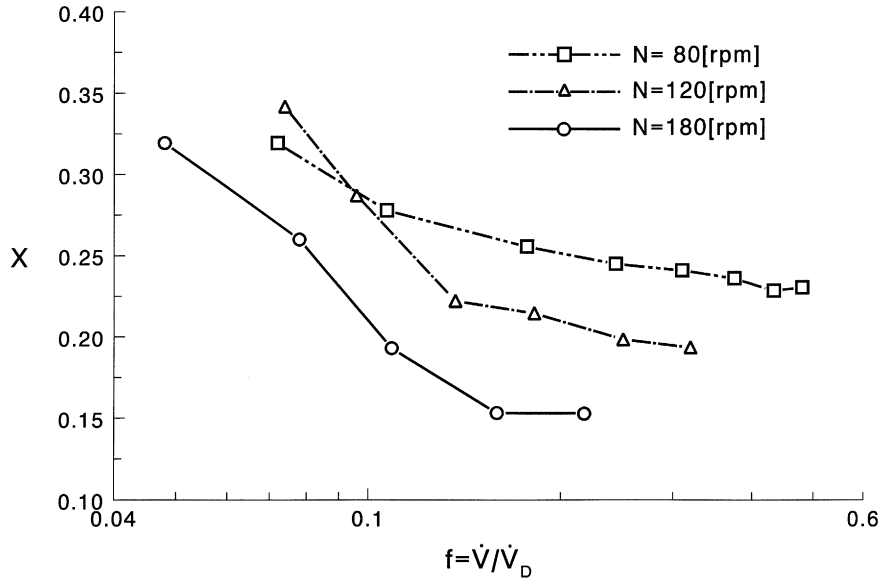

Fig. 12. Final selectivity of parallel reactions determined experimentally for a partially filled section of CoTSE; $\dot{V}_{BC}/\dot{V}_A = 24$.

created on the flights surface. Hence, the initial thickness of the side stream could be estimated from the following expression:

$$s_0 \cong \frac{\dot{V}_A}{\dot{V}_A + \dot{V}_{BC}} wf = \frac{w}{1 + \dot{V}_{BC}/\dot{V}_A} \frac{\dot{V}}{\dot{V}_D}. \quad (49)$$

In the computations this value was additionally increased by the factor of two because in the initial stages of mixing only one side of the NaOH-rich layer contacts the acid and ester solution. The average rate of deformation in the reaction zone was determined for experimental points reported in Fig. 12 by fitting the predicted by the model selectivity of the parallel reactions to the selectivity determined experimentally.

The dimensionless average rates of deformation, $\langle\alpha\rangle/N$, obtained in the fitting procedure for various degrees of fill, f, are plotted in Fig. 13. These results clearly show that decreasing the degree of fill, f, performed without changing the screw speed, N, decreases the ratio $\langle\alpha\rangle/N$. This effect is very strong for the higher screw speeds and $f < 0.2$ when no flow disturbances were observed. It should be noted that the values of $\langle\alpha\rangle/N$ obtained for the lowest degrees of fill for each screw speed, when the selectivity exceeded 30% and the initial striation thickness, s_0, ranged between 0.01 and 0.1 mm,

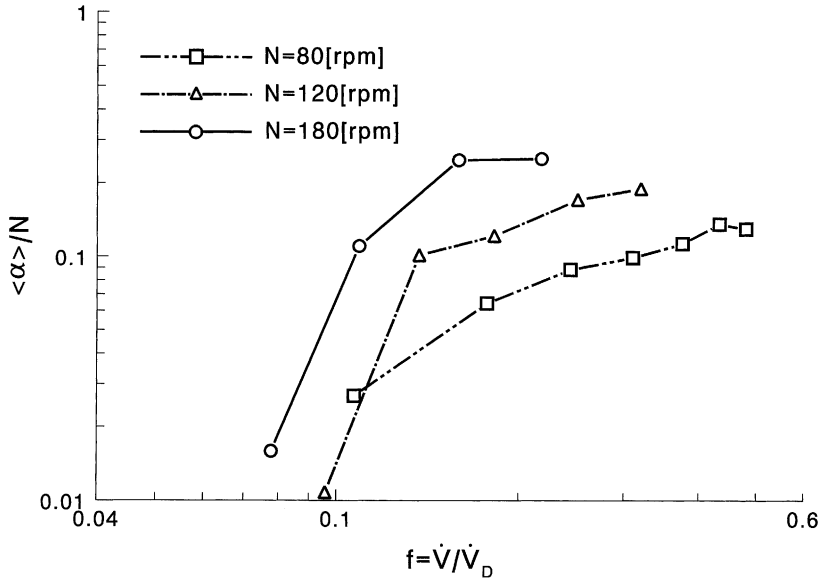

Fig. 13. Average rate of deformation identified for a partially filled section of CoTSE.

were found to be of the order of 10^{-3} or lower. In these circumstances the ratio of characteristic times of molecular diffusion and deformation $\theta_2 = t_D/t_F$, ranged between 10^{-3} and 10^{-4}. At such low values of θ_2 mixing at the molecular scale and chemical reactions proceeding between initially segregated substrates occurs in the diffusion-controlled regime with all its consequences, e.g. higher conversion of valuable substrates in slower side-reactions.

Remarkably, the average rates of deformation obtained for the highest degrees of fill of the extruder channel are comparable or even higher than those determined for the completely filled channel, compare Figs. 11 and 13.

To sum it up one should be aware that the reduction of the degree of fill in the feeding section of CoTSE below 8–10% results in a severe deterioration of the mixing conditions. This in turn significantly changes the course of the instantaneous and fast chemical reactions proceeding between the contacted reactants before the processed material can reach the fully filled mixing section of the extruder.

5. Conclusions

A new version of the model of laminar micromixing developed by Bałdyga et al. [10] has been worked out. Similarly as in the previous formulation viscous deformation of fluid elements and molecular diffusion, accelerated by the growth of the contact area between mixed liquids and reduction of segregation scales in a system, were recognised as the processes responsible for homogenisation at the molecular scale. Micromixing accompanied by an instantaneous or a fast chemical reaction was described in a local frame of reference. An integral transformation was applied to the material balance to obtain relations for concentration moments determining the quantity and characterising the spatial distribution of the reactants. Integral reaction terms in the model equations were estimated by means of continuous algebraic approximations of the local concentration profiles of the reactants instead of assuming, as it was done previously, a uniform distribution of one of the reactants in the reaction zone.

The model has been tested by comparison of model results obtained for the parallel reactions proceeding between unmixed reactants in elongated fluid striations with the direct numerical solution of material balance equations. This allowed to adjust the approximations of the local concentration profiles so that the model could predict the final selectivity with a high accuracy. In contrast to the earlier model the application range of the new model is no more restricted to mixing of reactants of almost equal molecular diffusivities or mixing a small volume of a highly concentrated solution of one reactant with a large volume of a diluted premixture of other reactants. Even if the molecular diffusivities of the reactants differ significantly and the initial concentration of the limiting reactant is twice higher than the concentrations of other reactants the accuracy of the model is high. Remarkably, the wide application range and the high accuracy was achieved without a significant increase of the model complexity and the computation cost than that required previously.

A system of competitive-parallel reactions and a viscosity increasing agent has been used in an experimental study of micromixing in a co-rotating twin-screw extruder. In this work the effect of the screw speed, the extruder throughput, the volume ratio of the reactant solutions and the degree of fill of the extruder, on the final selectivity of the test reactions was determined. The experimental results prove that the influence of micromixing on the course of complex chemical reactions carried out between initially unmixed reactants can not be neglected in the reactive extrusion technology.

The micromixing model has been used to interpret the experimental results. The values of the average rate of deformation of fluid elements in the extruder channel were determined for a broad range of: the screw speeds, the extruder throughputs and the degrees of fill of the extruder. It was found that in a completely filled section mechanical mixing could be intensified not only by increasing the screw speed but also by increasing the ratio of the real throughput to the maximum flow capacity. In the partially filled channel the degree of fill and the screw speed were found to be the key factors affecting micromixing. Increasing the degree of fill of the extruder and the screw speed increase the rate of viscous deformation. If the degree of fill is too low (in our case less than 8–10%) mixing occurs mainly due to molecular diffusion. Then the slower side reactions can proceed at rates comparable to the rate of the very fast or fast reaction and deteriorate the product quality.

Acknowledgements

The authors would like to thank Dr. P.H.M. Elemans for his suggestion to conduct the experimental part of this study and for organising a financial support of the DSM Research in Geleen, The Netherlands.

The access to the Cray J932 supercomputer at The University of Groningen, The Netherlands, would not be possible without a kind assistance of Prof. L.L. van Dierendonck, Prof. L.P.B.M. Janssen and funds received from The Dutch School of the Process Technology (OSPT).

References

[1] E.B. Nauman, B.A. Buffham, Mixing in Continous Flow Systems, Wiley, Chichester, UK, 1983.
[2] J. Bałdyga, J.R. Bourne, in: N.P. Cheremisinoff (Ed.), Encyclopedia of Fluid Mechanics, Vol. 1, Gulf Publishing, Houston, TX, 1986, pp. 147–199.
[3] S.D. Fields, J.M. Ottino, Chem. Eng. Sci. 42 (1987) 467–477.
[4] J. Bałdyga, J.R. Bourne, Turbulent Mixing and Chemical Reactions, Wiley, Chichester, UK, 1999.
[5] R.S. Spencer, R.M. Wiley, J. Colloid Sci. 6 (1951) 133–145.
[6] W.D. Mohr, in: E.C. Bernhardt (Ed.), Processing of Thermoplastic Materials, Reinhold, New York, 1959, pp. 117–152.

[7] L. Erwin, Polym. Eng. Sci. 18 (1978) 1044–1048.
[8] W.E. Ranz, AIChE J. 25 (1979) 41–47.
[9] J.M. Ottino, W.E. Ranz, C.W. Macosko, Chem. Eng. Sci. 34 (1979) 877–890.
[10] J. Bałdyga, A. Rozeń, F. Mostert, Chem. Eng. J. 69 (1998) 7–20.
[11] H.P. Grace, Chem. Eng. Commun. 14 (1981) 225–277.
[12] W.E. Ranz, AIChE J. 28 (1982) 91–96.
[13] J.R. Saylor, K.R. Sreenivasan, Phys. Fluids 10 (1998) 1135–1146.
[14] G. Tryggvason, W.J.A. Dahm, Combust. Flame 83 (1991) 207–220.
[15] A. Rozeń, Investigation of micromixing in very viscous liquids, Ph.D. Thesis, Warsaw University of Technology, Warszawa, Poland, 1995.
[16] C.J. Rauwendaal, Polym. Eng. Sci. 21 (1981) 1092–1100.
[17] P.H.M. Elemans, H.E.H. Meijer, in: N.P. Cheremisinoff (Ed.), Encyclopedia of Fluid Mechanics, Vol. 9, Gulf Publishing, Houston, TX, 1990, pp. 361–371.
[18] D.B. Todd, Polym. Eng. Sci. 15 (1975) 437–443.
[19] Y. Li, A. Senouci, R.A. Lai-Fook, A.C. Smith, Plast. Rubb. Proc. Appl. 11 (1989) 207–214.
[20] H.E.H. Meijer, P.H.M. Elemans, Polym. Eng. Sci. 28 (1988) 275–290.
[21] W. Michaeli, A. Grefenstein, U. Berghaus, Polym. Eng. Sci. 35 (1995) 1485–1504.
[22] K.J. Ganzeveld, L.P.B.M. Janssen, Polym. Eng. Sci. 32 (1992) 457–466.
[23] A.M. Donn, Micromixing in twin-screw extruders with neutral kneading discs, Ph.D. Thesis, University of Delaware, 1993.
[24] J.-C. Wu, Micromixing of a polymer melt in twin-screw extruders with kneading discs, Ph.D. Thesis, University of Delaware, 1994.
[25] J. Frey, C.D. Denson, Chem. Eng. Sci. 43 (1988) 1967–1973.
[26] R.A. Graaf, The use of twin screw extruders as starch modification reactors, Ph.D. Thesis, State University of Groningen, 1996.
[27] T. Meyer, A. Renken, Chem. Eng. Sci. 45 (1990) 2793–2800.
[28] W.F. Riley, L.D. Sturges, Engineering Mechanics, Dynamics, Wiley, New York, 1993.
[29] J. Bałdyga, J.R. Bourne, Chem. Eng. Sci. 45 (1990) 907–916.
[30] M.L. Booy, Polym. Eng. Sci. 20 (1980) 1220–1228.
[31] C.D. Denson, B.K. Hwang, Polym. Eng. Sci. 20 (1980) 965–971.